ENVIRONMENTAL RESEARCH
LETTERS

LETTER • OPEN ACCESS

A monitoring and prediction system for compound dry and hot events

To cite this article: Zengchao Hao *et al* 2019 *Environ. Res. Lett.* **14** 114034

Environmental Research Letters

LETTER

A monitoring and prediction system for compound dry and hot events

Zengchao Hao[1], Fanghua Hao[1], Youlong Xia[2], Vijay P Singh[3] and Xuan Zhang[1]

[1] College of Water Sciences, Beijing Normal University, Beijing 100875, People's Republic of China
[2] I.M. System Group at Environmental Modeling Center, National Centers for Environmental Prediction, College Park, Maryland, United States of America
[3] Department of Biological and Agricultural Engineering and Zachry Department of Civil Engineering, Texas A&M University, College Station, TX 77843-2117, United States of America

E-mail: haozc@bnu.edu.cn

Keywords: compound event, dry and hot, monitoring, prediction

Supplementary material for this article is available online

OPEN ACCESS

RECEIVED
3 July 2019

REVISED
1 October 2019

ACCEPTED FOR PUBLICATION
15 October 2019

PUBLISHED
14 November 2019

Abstract

Compound dry and hot events (i.e. concurrent or consecutive occurrences of dry and hot events), which may cause larger impacts than those caused by extreme events occurring in isolation, have attracted wide attention in recent decades. Increased occurrences of compound dry and hot events in different regions around the globe highlight the importance of improved understanding and modeling of these events so that they can be tracked and predicted ahead of time. In this study, a monitoring and prediction system of compound dry and hot events at the global scale is introduced. The monitoring component consists of two indicators (standardized compound event indicator and a binary variable) that incorporate both dry and hot conditions for characterizing the severity and occurrence. The two indicators are shown to perform well in depicting compound dry and hot events during June–July–August 2010 in western Russia. The prediction component consists of two statistical models, including a conditional distribution model and a logistic regression model, for predicting compound dry and hot events based on El Niño–Southern Oscillation, which is shown to significantly affect compound events of several regions, including northern South America, southern Africa, southeast Asia, and Australia. These models are shown to perform well in predicting compound events in large regions (e.g. northern South America and southern Africa) during December–January–February 2015–2016. This monitoring and prediction system could be useful for providing early warning information of compound dry and hot events.

1. Introduction

Droughts and hot extremes may cause severe impacts on the society and ecosystem (Mishra and Singh 2011, Perkins *et al* 2012, Coumou and Robinson 2013, Russo *et al* 2016, Oliver *et al* 2018). These two extremes are interconnected and may occur concurrently or consecutively (i.e. compound dry and hot events) (Seneviratne *et al* 2012, Leonard *et al* 2014, Liu *et al* 2017, Miralles *et al* 2018, Russo *et al* 2019). Recent decades have witnessed multiple compound dry and hot events in different regions, such as Europe (2003), China (2006), Russia (2010), southern US (2011), and southern Africa (2015–2016) (Barriopedro *et al* 2011, Hoerling *et al* 2013, Flach *et al* 2018, Herring *et al* 2018, Wu *et al* 2019). The compound dry and hot event may lead to impacts larger than the sum of impacts from individual extremes and has attracted increased attention in recent decades (Seneviratne *et al* 2012, Kopp *et al* 2017, Zscheischler and Seneviratne 2017, Cheng *et al* 2019).

Numerous studies have analyzed the variability of compound dry and hot events through observations and model projections and highlighted increased occurrences of compound events (Beniston 2009, Hao *et al* 2013, Mazdiyasni and AghaKouchak 2015, Sharma and Mujumdar 2017, Zhou and Liu 2018, Chen *et al* 2019). For example, Zscheischler and

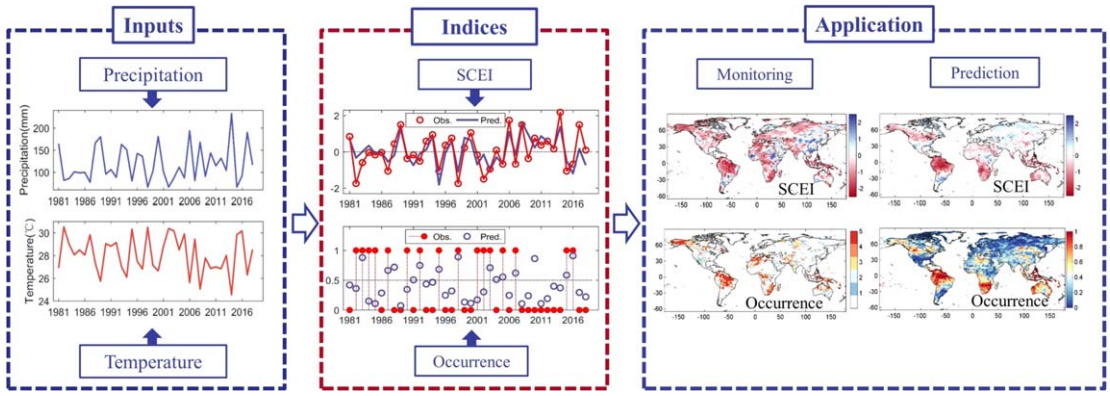

Figure 1. The framework of the global monitoring and prediction system of compound dry and hot events.

Seneviratne (2017) showed an increased likelihood of hot and dry seasons in many regions (e.g. southern Africa and central Europe), which may result from both the warming trend and the strengthened dependence between precipitation and temperature. Zhou and Liu (2018) investigated the likelihood of compound extremes in China based on the copula model and found increased occurrences of compound hot and dry events in the warm season over southwestern and northeastern China. The increased occurrences and large impacts of compound dry and hot events in different regions across the globe call for improved understanding of underlying mechanisms as well as reliable early warning. Since both dry and hot events may result from large scale global circulations, compound dry and hot events have been shown to be linked to common forcing factors (e.g. El Niño–Southern Oscillation, or ENSO) (López-Moreno *et al* 2011, Seneviratne *et al* 2012, Kopp *et al* 2017). Previous studies have explored the potential predictability of compound dry and hot events based on ENSO. For example, Hao *et al* (2019) proposed to employ the meta-Gaussian model for the prediction of compound events in southern Africa based on ENSO.

Due to large impacts of droughts and hot extremes, a variety of information systems at regional and global scales have been established for the monitoring and prediction of these events (Beguería *et al* 2010, Vicente-Serrano *et al* 2010, Hao *et al* 2014, Nijssen *et al* 2014, Yuan *et al* 2015, Zink *et al* 2016). For example, based on the standardized precipitation evapotranspiration index (SPEI), a global drought monitoring system has been developed to track drought conditions over global land areas (https://spei.csic.es/map/) (Beguería *et al* 2010, Vicente-Serrano *et al* 2010). Yuan *et al* (2015) developed the Princeton global seasonal hydrologic forecast system for hydrologic drought forecasting based on climate forecast and variable infiltration capacity model. Zink *et al* (2016) developed an online platform for drought monitoring in Germany based on soil moisture estimate of the root zone from a hydrologic model on a daily basis. The large impacts from compound dry and hot events highlight the necessity to track their conditions and predict their occurrences ahead of time; however, an information system for monitoring and predicting compound dry and hot events is still lacking.

The objective of this study is to develop a monitoring and prediction system of compound dry and hot events at the global scale. Data and methods for the development of the system are introduced in section 2. Results of monitoring and prediction are presented in section 3, followed by the discussion and conclusion in section 4.

2. Monitoring and prediction system

In the study, a compound dry and hot event is defined based on monthly precipitation and temperature to illustrate different components of the system. The standardized compound event indicator (SCEI) and a binary variable are used for characterizing compound events at the global scale. The prediction component consists of predicting the severity (i.e. SCEI) and occurrence (i.e. the binary variable) based on the conditional distribution model and logistic regression model, respectively (Hao *et al* 2018a, Hao *et al* 2019). The framework of different components of the system is summarized in figure 1 and will be introduced in detail in the following sections.

2.1. Data

Global precipitation and temperature data were obtained from the reanalysis product of modern-era retrospective analysis for research and applications, version 2 (MERRA-2), which provides global estimates of land surface conditions for the period 1980—present at a spatial resolution of 0.5° × 0.625° (Gelaro *et al* 2017, Reichle *et al* 2017a). This dataset has been shown to perform better than its previous versions and is thus selected in this study (for the period 1980–2018). Two types of precipitation products are available in the MERRA-2 system (one is generated by atmospheric models and the other is corrected based

on observations). The corrected MERRA-2 precipitation, which involves merger and disaggregation of observational products and model estimates, were used in this study (Reichle *et al*, 2017b). Another dataset of global monthly precipitation and temperature from 1951 to 2016 at 0.5° spatial resolution was obtained from the climatic research unit (CRU) (Harris *et al* 2014). This dataset provides a relatively longer record of precipitation and temperature to extract compound dry and hot events and is also used in this study.

The Niño 3.4 Sea Surface Temperature (SST) index (NINO34), defined as the area averaged SST from 5S-5N and 170–120 W, was used as the ENSO indicator for the prediction of compound dry and hot events. In addition, indices of Pacific Decadal Oscillation (PDO) and North Atlantic Oscillation (NAO) were also used for analyzing their impacts on compound dry and hot events. These data were obtained from the Global Climate Observing System (GCOS) Working Group on Surface Pressure (WG-SP) (https://esrl.noaa.gov/psd/gcos_wgsp/Timeseries/).

2.2. Indicators and monitoring component

The drought condition was characterized by the standardized precipitation index (SPI) based on accumulated precipitation of different time scales (e.g. 3 month) (McKee *et al* 1993). The standardized temperature index (STI) was employed to assess the hot condition and was computed in a similar way to the SPI. Usually, a distribution function was fitted to precipitation (or temperature) to estimate the marginal probability, which was then transformed to a standardized index based on the standard normal distribution. To avoid assumptions of distribution forms, the empirical Gringorten plotting position (Gringorten 1963) was employed to estimate marginal probabilities and compute the SPI and STI based on precipitation and temperature of June–July–August (JJA) and December–January–February (DJF) (i.e. 3 month time scale) for the period from 1980 to 2018. Specifically, the empirical probability for each period i based on observations of sample size n was estimated as: $P(x_i) = (m_i - 0.44)/(n + 0.12)$, where m_i is the number of occurrences $x_k \leq x_i\,(1 \leq k \leq n)$. To facilitate statistical modeling, the NINO34 was also transformed into a standardized index (i.e. SNINO) using the same method.

A compound dry and hot event was defined by low precipitation (i.e. low SPI) and high temperature (i.e. high STI) of the same period. Two types of indicators of compound dry and hot events were defined in this system. The first indicator is the SCEI derived from the bivariate distribution function of precipitation (X) and temperature (Y) (or SPI and STI) (Hao *et al* 2019). Specifically, the joint probability distribution of low precipitation and high temperature can be expressed as:

$$P(X \leqslant x,\, Y > y) = P(X \leqslant x) - P(X \leqslant x,\, Y \leqslant y). \tag{1}$$

A variety of distribution families for estimating the distribution in equation (1), such as copula (Genest and Favre 2007, Liu *et al* 2015), have been used for deriving the joint distribution of compound events (Bevacqua *et al* 2017, Zscheischler *et al* 2017, Ribeiro *et al* 2019). To avoid the assumption of bivariate distribution forms, we derive the joint probability in equation (1) following the concept of Gringorten plotting position as follows:

$$P(x_i, y_i) = \frac{n_i - 0.44}{n + 0.12}, \tag{2}$$

where n is the length of observations; n_i is the number of occurrences $x_k \leqslant x_i$ and $y_k > y_i\,(1 \leqslant k \leqslant n)$.

Since the joint probability in equation (1) is not uniformly distributed, an empirical distribution F (based on the Gringorten plotting position) can be fitted to the joint probability to remap it into the uniform space (Mo and Lettenmaier 2014). Following the similar methodology in computing the SPI in the univariate case, the standardized index of compound dry and hot event can be derived by transforming the remapped joint probability through the standard normal distribution Φ. Specifically, the SCEI based on the joint probability of precipitation and temperature can then be expressed as (Hao *et al* 2019).

$$\mathrm{SCEI} = \Phi^{-1}(F(P(X \leqslant x,\, Y > y))). \tag{3}$$

Lower SCEI values indicate more severe conditions of compound dry and hot events. The advantage of this indicator is that it can be used to characterize the severity of a compound dry and hot event.

The second indicator is a binary variable ($Z = 1$ for occurrence and $Z = 0$ for non-occurrence), which indicates the occurrence based on precipitation (P) and temperature (T) (or based on SPI and STI). For specific thresholds p_0 and t_0 of precipitation and temperature, respectively, the occurrence of a compound dry and hot event can be expressed as:

$$Z = \begin{cases} 1, & P \leqslant p_0,\, T > t_0 \\ 0, & \text{otherwise} \end{cases}. \tag{4}$$

This indicator can be obtained simply by assessing the concurrence of low precipitation and high temperature for a specific period. For example, a compound dry and hot event can be defined to occur (i.e. $Z = 1$) when precipitation is lower than or equal to the 50th percentile ($P \leqslant P_{50}$) and temperature is higher than the 50th percentile ($T > T_{50}$). However, it falls short in characterizing severity, since there are only two values (1 for occurrence and 0 for nonoccurrence). To alleviate this shortcoming, we defined five thresholds of precipitation and temperature based on different percentiles, including P_{50}/T_{50}, P_{40}/T_{60}, P_{30}/T_{70}, P_{20}/T_{80}, and P_{10}/T_{90}, for each period JJA and DJF for each grid. The compound event was classified into 5 categories based on these five levels of occurrences for

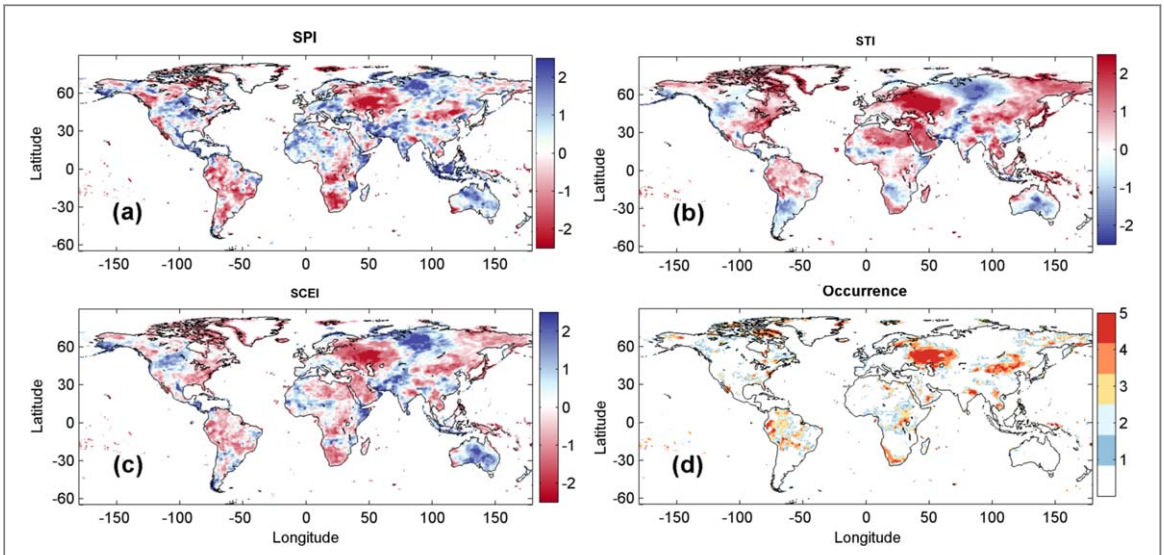

Figure 2. Monitoring of compound dry–hot conditions for the period June–July–August (JJA) of 2010 at the global scale. (a) SPI. (b) STI. (c) SCEI. (d) Occurrences based on different thresholds (1–5 in the color bar indicates the occurrence based on the thresholds P_{50}/T_{50}, P_{40}/T_{60}, P_{30}/T_{70}, P_{20}/T_{80}, and P_{10}/T_{90}, respectively).

characterizing compound dry and hot conditions. When the threshold value becomes extreme (e.g. from P_{50}/T_{50} to P_{10}/T_{90}), the number of occurrences generally decreases (figure S1 is available online at stacks.iop.org/ERL/14/114034/mmedia). The occurrence of a compound event based on the threshold P_{10}/T_{90} indicates more severe conditions than that based on the threshold P_{50}/T_{50}.

2.3. Prediction component

2.3.1. Conditional distribution model

The SCEI was used as the predictand for predicting the severity based on antecedent SCEI and SNINO, which represents the persistence and external forcing, respectively (Hao *et al* 2019). Specifically, the 1 month lead prediction of SCEI for a period t (W_{t+1}) can be achieved based on the conditional distribution given two predictors W_t and X_t (SNINO) which can be expressed as:

$$P(W_{t+1}|W_t, X_t). \tag{5}$$

By assuming a multivariate normal distribution of the three standardized variables (SPI, STI, and SNINO), the conditional distribution in equation (5) is essentially a normal distribution with mean μ and variance σ^2 (Wilks 2011, Hao *et al* 2019). The conditional mean μ can be regarded as the predicted severity of the compound event. The Pearson correlation coefficient between observed and predicted SCEI was used to evaluate the prediction skill of the conditional distribution model.

2.3.2. Logistic regression model

For the prediction of occurrences of compound events ($Z = 1$), the logistic regression model was employed and can be expressed as (Hao *et al* 2018a):

$$\ln\left[\frac{\pi}{1-\pi}\right] = \alpha + \beta\, x, \tag{6}$$

where π is the probability of occurrence $P(Z = 1|x)$; α is the constant and β is the regression coefficient; x is the predictor (i.e. NINO34). The 1 month lead prediction of the probability of occurrences of a compound dry and hot event (i.e. $Z = 1$) can then be expressed as:

$$P(Z_{t+1} = 1|x) = \frac{1}{1 + \exp[-(\alpha + \beta x_t)]}. \tag{7}$$

The Brier Skill Score (BSS) was used to evaluate the probabilistic prediction skill of the logistic regression model, which was defined as (Wilks 2011, Lepore *et al* 2017):

$$\mathrm{BSS} = 1 - \frac{\sum_{i=1}^{n}(P_i - O_i)^2}{\sum_{i=1}^{n}(R_i - O_i)^2}, \tag{8}$$

where n is the number of periods (or instances) of prediction; P_i is the predicted probability for period i; $O_i = 1$ if the compound event in observations occurs and $O_i = 0$ otherwise; R_i is the reference prediction, which is defined as the climatology frequency of occurrences of compound dry and hot events during the period 1980–2018. The BSS ranges from $-\infty$ to 1 with a positive value indicating skillful prediction (i.e. better prediction performance than the reference prediction).

3. Results

3.1. Monitoring of compound dry and hot events

The compound dry and heat wave event during 2010 summer in Russia (Barriopedro *et al* 2011, Zscheischler *et al* 2018), which is among the most severe compound dry and hot events in historical records, was used to illustrate the monitoring component of the system. The individual SPI and STI during JJA 2010 at the global

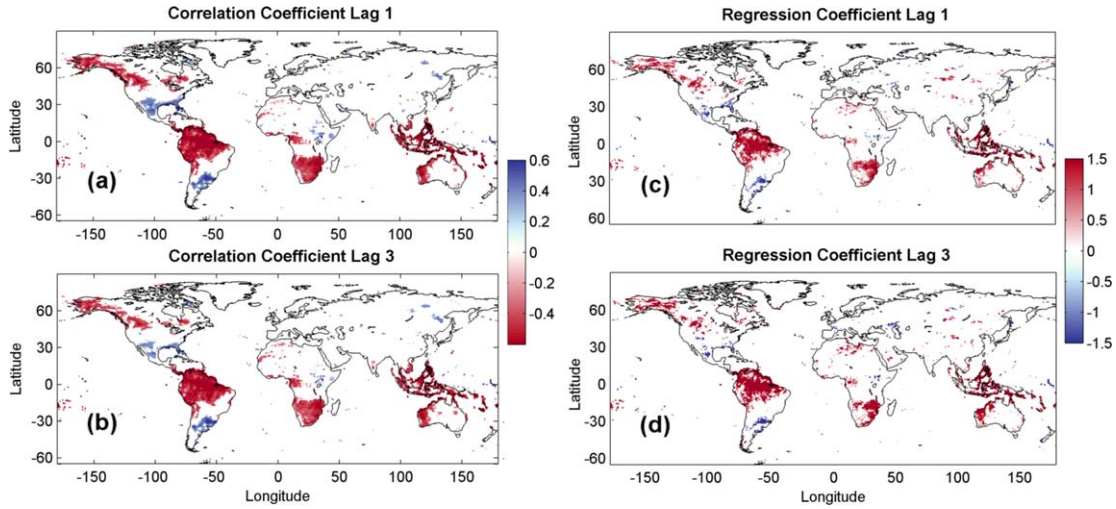

Figure 3. The correlation coefficient between SCEI and NINO34 for DJF (a), (b) and the logistic regression coefficient for DJF (c), (d) for lag-1 month and lag-3 month at the global scale.

scale is shown in figures 2(a), (b). Lower SPI and high STI values during JJA in western Russia (and eastern Europe) indicate severe dry and hot conditions. The monitoring of this compound event based on SCEI is shown in figure 2(c). The SCEI values were around −1.5 to −2.5 for large regions in western Russia (and eastern Europe), indicating severe conditions of compound dry and hot events. The monitoring of the occurrence of this compound event based on 5 combinations of thresholds is shown in figure 2(d). Occurrences of compound events exceeding the P_{10}/T_{90} threshold during this period were shown for large regions of western Russia, implying severe conditions of this compound dry and hot event. Other regions with lower values of SCEI and different levels of occurrences included parts of India and northern China, where concurrent droughts and high temperature anomalies during summer 2010 have been shown in previous studies (Schubert *et al* 2014, Panda *et al* 2017). We also assessed other historical occurrences of compound dry and hot events and overall the two indicators performed well in identifying historical compound events (not shown).

3.2. Prediction of the severity and occurrence

3.2.1. Predictor assessment

ENSO is a commonly used predictor for precipitation and temperature extremes across the globe and it tends to peak in boreal winter (Neelin *et al* 2000, Wang *et al* 2012, Yeh *et al* 2018). Thus, we focused on the prediction of compound dry and hot events during DJF. In this section, we assessed the validity of ENSO as the predictor by investigating its impact on compound dry and hot events during DJF. The lag 1 month and 3 month correlation coefficient (r) between SCEI of DJF and NINO34 in previous seasons (i.e. November–December–January (NDJ), September–October–November (SON)) is shown in figures 3(a), (b). Significant (and negative) correlation coefficients (at the 0.05 significance level) were found in large regions, including northern North America, northern South America, southern Africa, southeast Asia, and parts of Australia. This implies that lower SCEI values (or more severe compound event conditions) are associated with higher values of SNINO during DJF (or El Niño).

We used the threshold P_{50}/T_{50} to define the occurrence of compound dry and hot events. This setting enables the extraction of a relatively large number of occurrences for statistical modeling of compound events. Significant (and positive) regression coefficients β (at the 0.05 significance level) of lag 1 month and 3 month in equation (6) were used to assess the relationship between occurrences of compound events during DJF and NINO34 in previous seasons (NDJ and SON), which is shown in figures 3(c), (d). Similar to figures 3(a), (b), regions with significant (and positive) β mainly located in northern South America, southern Africa, southeast Asia, and parts of Australia. The positive values of β imply more occurrences of compound dry and hot events with higher values of NINO34 during DJF (or during El Niño years) in these regions.

For certain limited regions (e.g. southern North America), the opposite pattern of relationships between ENSO and compound events is shown (i.e. significant positive r and negative β). This indicates that La Niña (or low NINO34 values) is associated with increased occurrences of compound dry and hot events in southern North America. The main reason is that during La Niña, the Pacific jet stream often tends to shift northward, leading to dry and hot conditions in southern United States (Cook and Schaefer, 2008).

In previous sections, only 39 years of monthly precipitation and temperature data from MERRA-2 (i.e. 1980–2018) were used to evaluate the predictor. The number of compound dry and hot events extracted

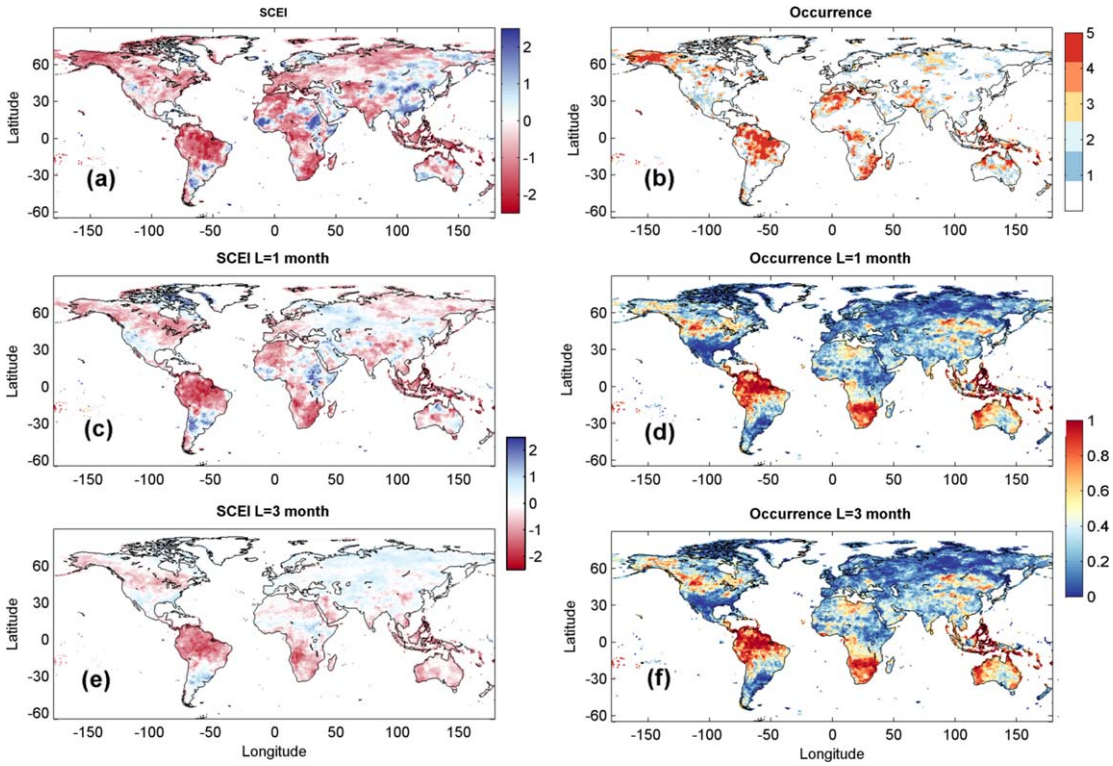

Figure 4. Observation and prediction (lead time $L = 1$ month and 3 months) of the compound dry and hot events of DJF 2016 at the global scale. (a) Observed SCEI; (b) observed occurrences based on different thresholds. (c), (e) 1 month and 3 month lead predictions of SCEI. (d), (f) 1 month and 3 month lead predictions of the occurrence based on the threshold P_{50}/T_{50}.

from historical records may not be sufficient for statistical modeling in certain regions. To address the potential uncertainty of datasets, we used the CRU data with a longer record (1951–2016) to assess ENSO impacts. The correlation coefficient (r) between SCEI and NINO34 and the regression coefficient (β) from the logistic regression model of lag 1 month and 3 month based on the CRU data are shown in figure S2. Overall, similar pattern of impacts of ENSO on compound dry and hot events is shown (negative r and positive β in regions such as northern South America and southern Africa). These results indicate that ENSO provides a good predictor for the prediction of compound events in these regions.

3.2.2. Model validation

To assess the prediction skill of the two prediction models, the leave-one-out cross validation (LOOCV) was used for the period from 1980 to 2018 ($n = 39$), in which the fitting procedure is repeated n times, each time with a sample of size $n-1$ by leaving out one sample for prediction and evaluation (Wilks 2011). For the prediction of SCEI, the positive correlation (significant at the 0.05 significance level) between observed and predicted SCEI values (1 month and 3 month lead time) of DJF during 1980–2018 based on LOOCV is shown in figure S3. Due to the persistence of SCEI, correlation coefficients between observations and 1 month lead predictions is high for large land areas. When the lead time increases to 3 month, high correlation coefficients between observations and predictions are mainly shown in southern US, northern South America, southern Africa, southeast Asia and parts of Australia. For the probabilistic prediction of occurrences, the BSS for the 1 month and 3 month lead prediction is shown in figure S4. Skillful predictions are shown in regions with significant relationships between ENSO and occurrences of compound dry and hot events (e.g. positive BSS values in northern South America and southern Africa). Overall, these results show that ENSO provides skillful prediction of compound events during DJF for 1 month and 3 month lead time for regions including southern US, northern South America, southern Africa, southeast Asia and parts of Australia.

3.2.3. Model application

Based on the analysis of the predictor and prediction skill above, we then applied the two models to predict compound events during DJF 2015–2016 as a case study. The monitoring of the compound event for this period is shown in figures 4(a), (b). From figure 4(a), the SCEI is particularly low in regions including northern South America, northern and southern Africa, southeast Asia, parts of Australia, and northern Russia. From figure 4(b), the occurrence of different categories of compound events resides in similar regions (e.g. occurrences in northern South America

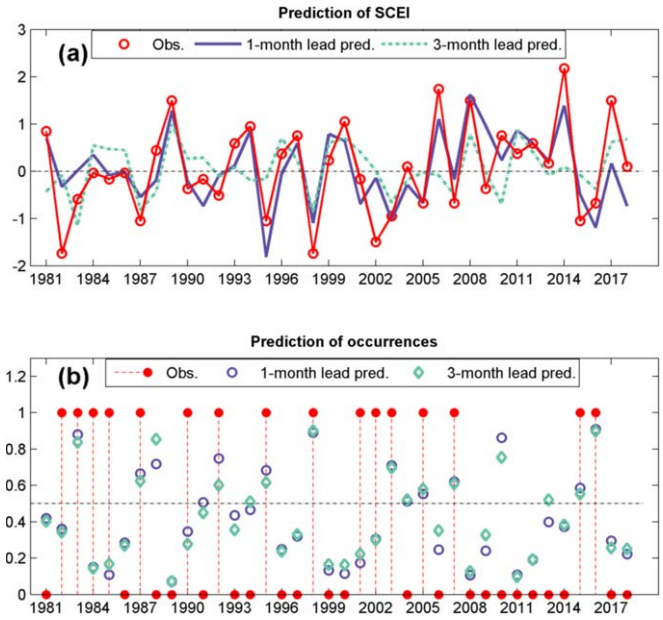

Figure 5. Illustration of the 1 month and 3 month lead prediction of the SCEI (a) and occurrence (b) of the compound dry and hot event for a grid in southern Africa based on leave-one-out cross validation (LOOCV).

and southern Africa based on the threshold P_{10}/T_{90}). These patterns of compound events are generally consistent with previous studies showing both drought and hot conditions for this period in these regions (Herring *et al* 2018), such as northern South America, southern Africa (Yuan *et al* 2018), and southeast Asia (King *et al* 2016, Christidis *et al* 2018).

The prediction of the SCEI and occurrence is first illustrated at one grid to show the application of the two models. The observed SCEI values and occurrences of compound events during DJF from 1980 to 2018 for one grid in southern Africa (longitude: 22.5, latitude: −20) are shown in figure 5, which indicates historical compound dry and hot events during certain periods, such as DJF 2015–2016. The 1 month and 3 month lead prediction of the SCEI and occurrence from the two models based on LOOCV is shown in figures 5(a) and (b), respectively. In figure 5(a), the correlation between observations and predictions of SCEI values is significant and relatively high (0.76 and 0.46 for 1 month and 3 month lead prediction, respectively). For the predicted probability of occurrences in figure 5(b), if 0.5 is selected as the threshold to define the occurrence, the probabilistic prediction from the logistic regression model performs well in identifying a large number of historical occurrences of compound events (e.g. during DJF 2015–2016). For example, the 1 month and 3 month lead prediction of the probability of occurrences of compound dry and hot events during DJF 2015–2016 is 0.91 and 0.90, respectively, indicating high likelihoods of occurrences during this period.

The 1 month and 3 month lead prediction of SCEI over global land areas is shown in figures 4(c), (e). The low SCEI values from the prediction generally resemble observations in figure 4(a) for large regions (e.g. northern South America, southern Africa, southeast Asia). In addition, the 1 month and 3 month lead prediction of occurrences is shown in figures 4(d), (f). Higher probability of occurrences of compound dry and hot events is predicted in similar regions to those with low SCEI values from the prediction in figures 4(c), (e), which is consistent with observed occurrences in figure 4(b). The relatively good prediction performance of compound dry and hot events for this period in these regions mainly results from the strong impact of ENSO (Hao *et al* 2019). However, the prediction model based on ENSO fails to predict compound dry and hot events in certain regions, such as northern Russia, where no significant impact of ENSO is shown from figure 3. These results highlight the useful early warning information of compound dry and hot events from this system for regions with significant impacts from ENSO. Meanwhile, improved understanding and modeling of compound events beyond the region significantly affected by ENSO is a pressing need to improve the system.

4. Discussion and conclusion

A global monitoring and prediction system for compound dry and hot events at the global scale is introduced in this study. The monitoring component consists of two indicators incorporating both dry and hot conditions, which is shown to perform well in depicting the compound event during summer 2010 in western Russia. For the prediction component, the conditional distribution model and logistic regression model are employed for predicting the severity and

occurrence of compound dry and hot events based on ENSO. These two models perform well in predicting the compound dry and hot event during DJF 2015–2016 in large regions (e.g. northern South America and southern Africa) for 1 month and 3 month lead time due to the strong impact of ENSO.

Though ENSO provides skillful prediction of compound dry and hot events, a significant relationship between ENSO and compound events exists only for certain global land areas. Thus, influences of other modes of climate variability (e.g. PDO and NAO) on compound events need to be assessed to improve the prediction of different regions. Similar to figure 3, we show the impact of PDO on compound dry and hot events based on lag 1 month and 3 month correlation coefficient (r) and regression coefficient (β) for DJF (significant at the 0.05 significance level) in figures S5 and S6 based on MERRA-2 and CRU data, respectively. High values of PDO tend to increase the likelihood of compound dry and hot events (negative r and positive β) in regions including northern North America, northern South America, part of Australia (Mantua and Hare 2002), which is roughly similar to the impact of ENSO. Similarly, based on MERRA-2 and CRU data, NAO is shown to affect compound dry and hot events in southern Europe and part of Mediterranean regions (figures S7, S8), which is consistent with previous studies (Brandimarte *et al* 2011, López-Moreno *et al* 2011). These results indicate that other modes of climate variability can be employed to improve the prediction of the system.

We mainly characterize compound dry and hot events based on two indicators incorporating precipitation and temperature at a monthly time scale. This method can be applied to more variables or indicators (e.g. SPEI) at finer time scales (e.g. define hot conditions based on heat wave). A potential limitation of the prediction component is that information of dry and hot conditions is combined into indicators while their joint status is not predicted explicitly. This can be alleviated by extending the conditional model in equation (5) to predict the joint distribution function of dry and hot conditions based on ESNO (Hao *et al* 2018b). In addition, the prediction of compound events is achieved based on statistical models, which rely on empirical relationships in historical records and generally fall short in capturing complicated physical processes. To address this limitation, seasonal prediction products from advanced general circulation models (or GCMs) (e.g. North American Multi-Model Ensemble) (Doblas-Reyes *et al* 2013, Mcevoy *et al* 2016, Wood *et al* 2015, Schubert *et al* 2016) could also be used for the prediction of compound dry and hot events to improve the performance in different regions. Results of this study will be available at the Global Compound Dry-hot Monitoring and Prediction System (GCDMaPS) website (gcdmaps.bnu.edu.cn). We stress that the purpose of this system is to provide alternatives to current efforts or systems in tracking droughts or hot extremes, such as the Global Drought Monitor (https://spei.csic.es/map/), with focus on compound events. This system could be useful for tracking and predicting compound dry and hot events at regional and global scales to reduce their potential impacts.

Acknowledgments

This research was funded by National Natural Science Foundation of China (Grant number 41601014). We thank the editor and reviewers for their constructive comments that help improve the manuscript. We are grateful for the Modern-Era Retrospective Analysis for Research and Applications, version 2 (MERRA-2) data provided by the Global Modeling and Assimilation Office (GMAO) at NASA Goddard Space Flight Center. We are thankful to the Climatic Research Unit for providing the CRU data. We also thank the global Climate Observing System (GCOS) Working Group on Surface Pressure (WG-SP) for providing climate indices.

Data availability statement

The data that support the findings of this study are openly available. Global monthly precipitation and temperature data of MERRA-2 from NASA Global Modeling and Assimilation Office are available at https://gmao.gsfc.nasa.gov/reanalysis/MERRA-2/. Global monthly precipitation and temperature data from the Climatic Research Unit (CRU) are available at http://cru.uea.ac.uk/data. Monthly climate indices (Niño 3.4, PDO, and NAO) from Global Climate Observing System (GCOS) Working Group on Surface Pressure (WG-SP) are available at https://esrl.noaa.gov/psd/gcos_wgsp/Timeseries.

ORCID iDs

Zengchao Hao https://orcid.org/0000-0001-7666-7053

References

Barriopedro D, Fischer E M, Luterbacher J, Trigo R M and García-Herrera R 2011 The hot summer of 2010: redrawing the temperature record map of europe *Science* **332** 220–4

Beguería S, Vicente-Serrano S M and Angulo-Martínez M 2010 A multiscalar global drought dataset: the SPEIbase: a new gridded product for the analysis of drought variability and impacts *Bull. Am. Meteorol. Soc.* **91** 1351–6

Beniston M 2009 Trends in joint quantiles of temperature and precipitation in Europe since 1901 and projected for 2100 *Geophys. Res. Lett.* **36** 07707

Bevacqua E, Maraun D, Hobæk Haff I, Widmann M and Vrac M 2017 Multivariate statistical modelling of compound events via pair-copula constructions: analysis of floods in Ravenna (Italy) *Hydrol. Earth Syst. Sci.* **21** 2701–23

Brandimarte L, Di Baldassarre G, Bruni G, D'Odorico P and Montanari A 2011 Relation between the north-Atlantic oscillation and hydroclimatic conditions in mediterranean areas *Water Resour. Manage.* **25** 1269–79

Chen L, Chen X, Cheng L, Zhou P and Liu Z 2019 Compound hot droughts over China: identification, risk patterns and variations *Atmos. Res.* **227** 210–9
Cheng L, Hoerling M, Liu Z and Eischeid J 2019 Physical understanding of human-induced changes in US hot droughts using equilibrium climate simulations *J. Clim.* **32** 4431–43
Christidis N, Manomaiphiboon K, Ciavarella A and Stott P A 2018 The hot and dry April of 2016 in Thailand *Bull. Am. Meteorol. Soc.* **99** S128–32
Cook A R and Schaefer J T 2008 The relation of El Niño–Southern Oscillation (ENSO) to winter tornado outbreaks *Mon. Wea. Rev.* **136** 3121–37
Coumou D and Robinson A 2013 Historic and future increase in the global land area affected by monthly heat extremes *Environ. Res. Lett.* **8** 034018
Doblas-Reyes F J, García-Serrano J, Lienert F, Biescas A P and Rodrigues L R L 2013 Seasonal climate predictability and forecasting: status and prospects *Wiley Interdiscip. Rev. Clim. Change* **4** 245–68
Flach M, Sippel S, Gans F, Bastos A, Brenning A, Reichstein M and Mahecha M D 2018 Contrasting biosphere responses to hydrometeorological extremes: revisiting the 2010 western Russian heatwave *Biogeosciences* **15** 6067–85
Gelaro R *et al* 2017 The modern-era retrospective analysis for research and applications, version 2 (MERRA-2) *J. Clim.* **30** 5419–54
Genest C and Favre A-C 2007 Everything you always wanted to know about copula modeling but were afraid to ask *J. Hydrol. Eng.* **12** 347–68
Gringorten I I 1963 A plotting rule for extreme probability paper *J. Geophys. Res.* **68** 813–4
Hao Z, AghaKouchak A, Nakhjiri N and Farahmand A 2014 Global integrated drought monitoring and prediction system *Sci. Data* **1** 140001
Hao Z, AghaKouchak A and Phillips T J 2013 Changes in concurrent monthly precipitation and temperature extremes *Environ. Res. Lett.* **8** 034014
Hao Z, Hao F, Singh V P, Xia Y, Shi C and Zhang X 2018b A multivariate approach for statistical assessments of compound extremes *J. Hydrol.* **565** 87–94
Hao Z, Hao F, Singh V P and Zhang X 2018a Quantifying the relationship between compound dry and hot events and El Niño–Southern Oscillation (ENSO) at the global scale *J. Hydrol.* **567** 332–8
Hao Z, Hao F, Singh V P and Zhang X 2019 Statistical prediction of the severity of compound dry–hot events based on El Niño-Southern Oscillation *J. Hydrol.* **572** 243–50
Harris I, Jones P D, Osborn T J and Lister D H 2014 Updated high-resolution grids of monthly climatic observations—the CRU TS3.10 Dataset *Int. J. Climatol.* **34** 623–42
Herring S C, Christidis N, Hoell A, Kossin J P III, Schreck C J and Stott P A 2018 Explaining extreme events of 2016 from a climate perspective *Bull. Am. Meteorol. Soc.* **99** S1–157
Hoerling M *et al* 2013 Anatomy of an extreme event *J. Clim.* **26** 2811–32
King A D, Karoly D J and Oldenborgh G J V 2016 Climate change and El Niño increase likelihood of indonesian heat and drought *Bull. Am. Meteorol. Soc.* **97** S113–7
Kopp R, Easterling D R, Hall T, Hayhoe K, Horton R, Kunkel K and LeGrande A 2017 Potential surprises–compound extremes and tipping elements *Climate Science Special Report: Fourth National Climate Assessment, Volume 1* ed D J Wuebbles *et al* (Washington DC: US Global Change Research Program) pp 411–29
Leonard M *et al* 2014 A compound event framework for understanding extreme impacts *Wiley Interdiscip. Rev. Clim. Change* **5** 113–28
Lepore C, Tippett M K and Allen J T 2017 ENSO-based probabilistic forecasts of March–May US tornado and hail activity *Geophys. Res. Lett.* **44** 9093–101
Liu X, Tang Q, Zhang X, Groisman P, Sun S, Lu H and Li Z 2017 Spatially distinct effects of preceding precipitation on heat stress over eastern China *Environ. Res. Lett.* **12** 115010
Liu Z, Zhou P, Chen X and Guan Y 2015 A multivariate conditional model for streamflow prediction and spatial precipitation refinement *J. Geophys. Res. Atmos.* **120** 10116–29
López-Moreno J I, Vicente-Serrano S M, Morán-Tejeda E, Lorenzo-Lacruz J, Kenawy A and Beniston M 2011 Effects of the North Atlantic Oscillation (NAO) on combined temperature and precipitation winter modes in the Mediterranean mountains: observed relationships and projections for the 21st century *Glob. Planet. Change* **77** 62–76
Mantua N J and Hare S R 2002 The pacific decadal oscillation *J. Oceanogr.* **58** 35–44
Mazdiyasni O and AghaKouchak A 2015 Substantial increase in concurrent droughts and heatwaves in the United States *Proc. Natl Acad. Sci.* **112** 11484–9
Mcevoy D J, Huntington J L, Mejia J F and Hobbins M T 2016 Improved seasonal drought forecasts using reference evapotranspiration anomalies *Geophys. Res. Lett.* **43** 377–85
McKee T B, Doesken N J and Kleist J 1993 The relationship of drought frequency and duration to time scales *Eighth Conf. on Applied Climatology, Am. Meteorol. Soc. (Anaheim, CA)*
Miralles D G, Gentine P, Seneviratne S I and Teuling A J 2018 Land–atmospheric feedbacks during droughts and heatwaves: state of the science and current challenges *Ann. New York Acad. Sci.* **1436** 19–35
Mishra A K and Singh V P 2011 Drought modeling-a review *J. Hydrol.* **403** 157–75
Mo K C and Lettenmaier D P 2014 Objective drought classification using multiple land surface models *J. Hydrometeorol.* **15** 990–1010
Neelin J D, Jin F-F and Syu H-H 2000 Variations in ENSO phase locking *J. Clim.* **13** 2570–90
Nijssen B, Shukla S, Lin C-Y and Lettenmaier D 2014 A prototype Global Drought Information System based on multiple land surface models *J. Hydrometeorolgy* **15** 1661–76
Oliver E C J *et al* 2018 Longer and more frequent marine heatwaves over the past century *Nat. Commun.* **9** 1324
Panda D K, AghaKouchak A and Ambast S K 2017 Increasing heat waves and warm spells in India, observed from a multiaspect framework *J. Geophys. Res. Atmos.* **122** 3837–58
Perkins S E, Alexander L V and Nairn J R 2012 Increasing frequency, intensity and duration of observed global heatwaves and warm spells *Geophys. Res. Lett.* **39** L20714
Reichle R H, Draper C S, Liu Q, Girotto M, Mahanama S P P, Koster R D and Lannoy G J M D 2017a Assessment of MERRA-2 land surface hydrology estimates *J. Clim.* **30** 2937–60
Reichle R H, Liu Q, Koster R D, Draper C S, Mahanama S P P and Partyka G S 2017b Land surface precipitation in MERRA-2 *J. Climate* **30** 1643–64
Ribeiro A F S, Russo A, Gouveia C M and Páscoa P 2019 Copula-based agricultural drought risk of rainfed cropping systems *Agric. Water Manage.* **223** 105689
Russo A, Gouveia C M, Dutra E, Soares P M M and Trigo R M 2019 The synergy between drought and extremely hot summers in the Mediterranean *Environ. Res. Lett.* **14** 014011
Russo S, Marchese A F, Sillmann J and Immé G 2016 When will unusual heat waves become normal in a warming Africa? *Environ. Res. Lett.* **11** 054016
Schubert S D *et al* 2016 Global meteorological drought: a synthesis of current understanding with a focus on SST drivers of precipitation deficits *J. Clim.* **29** 3989–4019
Schubert S D, Wang H, Koster R D, Suarez M J and Groisman P Y 2014 Northern Eurasian heat waves and droughts *J. Clim.* **27** 3169–207
Seneviratne S I *et al* 2012 Changes in climate extremes and their impacts on the natural physical environment *Managing the Risks of Extreme Events and Disasters to Advance Climate Change Adaptation. A Special Report of Working Groups I and II of the Intergovernmental Panel on Climate Change (IPCC)* ed C B Field *et al* (Cambridge: Cambridge University Press) pp 109–230

Sharma S and Mujumdar P 2017 Increasing frequency and spatial extent of concurrent meteorological droughts and heatwaves in India *Sci. Rep.* **7** 15582

Vicente-Serrano S M, Beguería S and López-Moreno J I 2010 A multiscalar drought index sensitive to global warming: the standardized precipitation evapotranspiration index *J. Clim.* **23** 1696–718

Wang H, Kumar A, Wang W and Jha B 2012 US summer precipitation and temperature patterns following the peak phase of El Niño *J. Clim.* **25** 7204–15

Wilks D S 2011 *Statistical Methods in the Atmospheric Sciences* (San Diego, CA.: Academic)

Wood E F, Schubert S D, Wood A W, Peters-Lidard C D, Mo K C, Mariotti A and Pulwarty R S 2015 Prospects for advancing drought understanding, monitoring and prediction *J. Hydrometeorol.* **16** 1636–57

Wu X, Hao Z, Hao F, Singh V P and Zhang X 2019 Dry–Hot magnitude index: a joint indicator for compound event analysis *Environ. Res. Lett.* **14** 064017

Yeh S-W *et al* 2018 ENSO atmospheric teleconnections and their response to greenhouse gas forcing *Rev. Geophys.* **56** 185–206

Yuan X, Roundy J K, Wood E F and Sheffield J 2015 Seasonal forecasting of global hydrologic extremes: system development and evaluation over GEWEX basins *Bull. Am. Meteorol. Soc.* **96** 1895–912

Yuan X, Wang L and Wood E F 2018 Anthropogenic intensification of southern African flash droughts as exemplified by the 2015/16 season *Bull. Am. Meteorol. Soc.* **99** S86–90

Zhou P and Liu Z 2018 Likelihood of concurrent climate extremes and variations over China *Environ. Res. Lett.* **13** 094023

Zink M, Samaniego L, Kumar R, Thober S, Mai J, Schäfer D and Marx A 2016 The German drought monitor *Environ. Res. Lett.* **11** 074002

Zscheischler J *et al* 2018 Future climate risk from compound events *Nat. Clim. Change* **8** 469–77

Zscheischler J, Orth R and Seneviratne S I 2017 Bivariate return periods of temperature and precipitation explain a large fraction of European crop yields *Biogeosciences* **14** 3309–20

Zscheischler J and Seneviratne S I 2017 Dependence of drivers affects risks associated with compound events *Sci. Adv.* **3** e1700263